

Preparation of Barium Titanate Films at 55°C by an Electrochemical Method

Priya Bendale, Sridhar Venigalla,* John R. Ambrose, Ellis D. Verink, Jr., and James H. Adair*

Department of Materials Science and Engineering, University of Florida, Gainesville, Florida 32611

Work by previous investigators has shown that BaTiO₃ films can be synthesized from solution over temperature ranges from 80°C to greater than 200°C. In the present work, electrically insulating crystalline films of BaTiO₃ have been electrochemically deposited on titanium substrates at temperatures as low as 55°C. Auger spectroscopic analyses with depth profiling indicate that a titanium oxide layer whose thickness is governed by current density acts as a precursor to BaTiO₃. Formation of BaTiO₃ is found to be favored only in highly alkaline solutions. This is consistent with the phase stability reported for the Ba-Ti-CO₂-H₂O system at 25°C. Lower processing temperatures (55°C) favor the formation of thick, electrically resistive, and well-crystallized BaTiO₃ films, apparently due to increased oxygen solubility in the electrolyte solution. Films produced at 100°C are much thinner and are electrically conductive due to fissures and pores in their microstructure. Initial studies on the effect of current density indicate the formation of thinner and porous films with thicker titanium oxide intermediate layers.

I. Introduction

THE preparation of thin films by electrochemical methods has the potential for the near-room-temperature production of multilayer capacitors, ferroelectric memories, surface acoustic wave devices, and ferroelectric field effect transistors, as well as for structural and environmental applications such as high-strength ceramic coatings for internal combustion and jet propulsion systems. Previous reports indicate that perovskite thin films such as BaTiO₃, CaTiO₃, and SrTiO₃ can be formed by a hydrothermal-electrochemical method.¹⁻⁶

Deposition or growth of sparingly soluble single-component oxides on metal surfaces is neither novel nor difficult to accomplish.⁷⁻¹¹ The process of anodization is achieved by anodic polarization of the metal surface to form the resistive metal oxide coating. Composition of the coating depends upon the composition of the metal and the solution in which the anodization is performed, with cationic and anionic species incorporated into the structure of the oxide. It is critical to ensure that the polarization-induced reactions proceed with sufficient singularity to assure that the desired reaction product is formed and that parallel or side reactions that result in formation of alternative compositions are avoided.

Preliminary experiments in the current work confirm the electrochemical synthesis of BaTiO₃. More significantly, BaTiO₃ thin films have been synthesized in aqueous solutions at temperatures as low as 55°C, thus eliminating the use of pressurized vessels. Attempts to form BaTiO₃ near 25°C have produced isolated deposits of an unknown material. Additional

research to synthesize BaTiO₃ thin films at temperatures approaching room temperature is in progress. In the present paper, the conditions and procedures required to achieve approximately 1- μ m-thick films at 55°C are presented, followed by an experimentally verifiable hypothesis for the formation mechanism.

II. Background and Approach

The general approach has been to develop methods that promote the synthesis of BaTiO₃ films at temperatures less than 100°C. Sealed pressure vessels are ordinarily required in hydrothermal synthesis for reaction temperatures at 100°C or greater to prevent boiling of the solution. Continuous processing is more efficient with open vessels at lower temperatures. Thus, lower synthesis temperatures make the overall process more feasible.

Prior work provides the fundamental understanding of the solution chemistry of the Ba-Ti-CO₂-H₂O system to develop procedures to produce BaCO₃-free BaTiO₃ thin films at low temperatures.^{12,13} As shown in the phase stability diagram in Fig. 1 for this system, BaTiO₃ is predicted to be the stable phase above about pH 12 if the pCO₂ is less than 4.5. With increased CO₂ concentration, BaCO₃ is the stable phase at pH values up to 13. Therefore, care must be exercised to exclude CO₂ if the ultralow temperature synthesis of BaTiO₃ is to be achieved as predicted.

Experimental work on hydrothermal synthesis and dissolution studies in solution verify that the phase stability theoretically predicted for BaTiO₃ at 25°C is valid.¹²⁻²⁶ The phase stability of a material in a particular solution is best determined by both precipitation and dissolution of the relevant material because reaction kinetics may be slow, particularly for the former phenomenon. Several studies have demonstrated that the dissolution behavior of BaTiO₃ at 25°C is consistent with the phase stability diagram in Fig. 1. BaTiO₃ measurably decomposes in aqueous solutions below pH 11 to either BaCO₃ or Ba²⁺ and a TiO₂-rich layer depending on the CO₂ concentration in solution.¹¹⁻¹⁴ In contrast, BaTiO₃ particles have been synthesized in aqueous solutions only at temperatures as low as 60°C.^{19,24} The reaction rates are sluggish for the hydrothermal synthesis of BaTiO₃ at low temperatures, and only nanometer-size particles are produced.^{19,24} However, it has been demonstrated that BaTiO₃ can be synthesized over a large range of temperatures, with reaction rate generally increasing with increasing temperature.¹⁵⁻²⁶

It is likely that the formation of BaTiO₃ from solution follows classical concepts of nucleation and growth from solution²⁷⁻²⁹ such that a sufficient degree of supersaturation as well as heterogeneous nucleation sites are necessary. Dissolution studies support the theoretical prediction that BaTiO₃ is the stable phase in alkaline aqueous solution at 25°C.¹³ The sluggish reaction rates and the inability to form particles from aqueous solution at temperatures below 60°C support the contention that the required levels of supersaturation of cationic species, particularly Ti⁴⁺, are not achieved in conventional precipitation. Thus, a key feature of the electrochemical process is that a heterogeneous surface with a high local chemical potential of the cationic species is provided for the formation of BaTiO₃. This

D. W. Johnson, Jr.—contributing editor

Manuscript No. 195586. Received June 18, 1992; approved November 24, 1992.

*Member, American Ceramic Society.

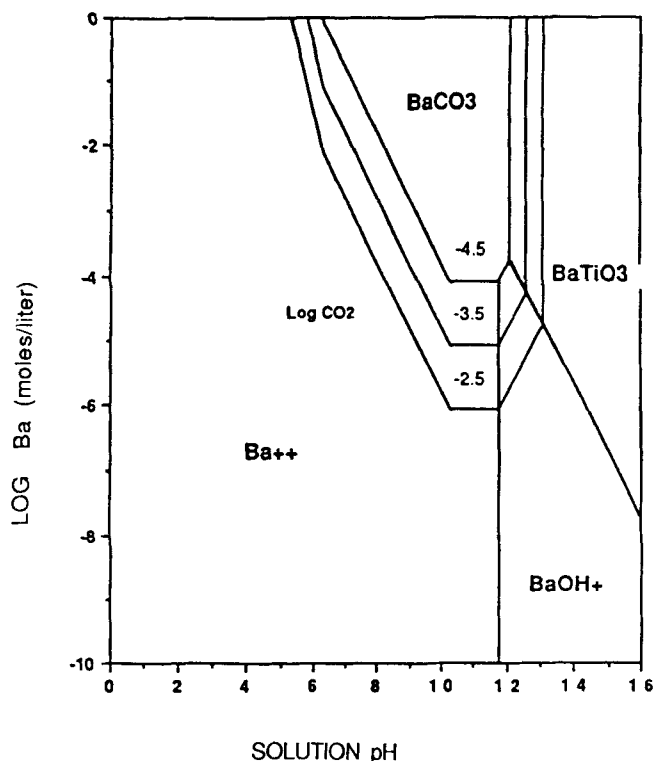


Fig. 1. Theoretical phase stability diagram for the system Ba-Ti-CO₂-H₂O system (Refs. 12 and 13).

observation may have implications in the formation of electrothermal films in other systems as well.

III. Materials and Methods

A schematic diagram of the experimental setup is shown in Fig. 2. Preliminary experiments were performed in a borosilicate vessel, but the highly alkaline solution pH values required for BaTiO₃ formation lead to etching of the glass. Therefore, a 1-L Teflon vessel was used in all reported experiments. All surfaces in contact with the electrolyte solution were either Teflon or platinum except the anode. The cathode and anode were a platinum plate and a titanium corrosion coupon, respectively. The titanium corrosion coupons (electronic grade, Johnson Matthey, Ward Hill, MA) (1.5 cm × 1.5 cm × 0.1 cm) were mechanically polished with alumina to 0.05 μm and degreased in ethanol (Fisher Scientific, Fair Lawn, NJ) prior to anodic deposition. (All chemicals are reagent grade unless otherwise indicated.) The electrodes were suspended from platinum wires and placed in a Teflon beaker containing the electrolyte. All experiments were performed under galvanostatic conditions (i.e., constant current) with the current density varied from 0 to 2.5 mA·cm⁻² with a commercial power source (Potentiostat Model 173, Princeton Applied Research, Princeton, NJ). Changes in potential as a function of reaction time were collected on a strip chart recorder for selected experiments. Since all experiments were conducted under galvanostatic conditions, it was not necessary to include a reference electrode in the apparatus. The atmosphere in the vessel was controlled by purging the solution with suitable gas (O₂ or N₂) using a gas dispersion tube made of Teflon. The flow rate for the gas through the solution was maintained between 1 and 10 cm³·min⁻¹ for all experiments.

Details for each of the experiments are outlined in Table I. Preliminary experiments indicated that the formation of BaTiO₃ required solution pH values greater than pH 12.5. Ba²⁺ in 0.5M concentration as either Ba(OH)₂·8H₂O or Ba(CH₃COO)₂, the acetate salt, was used to assess the effect of the source of the

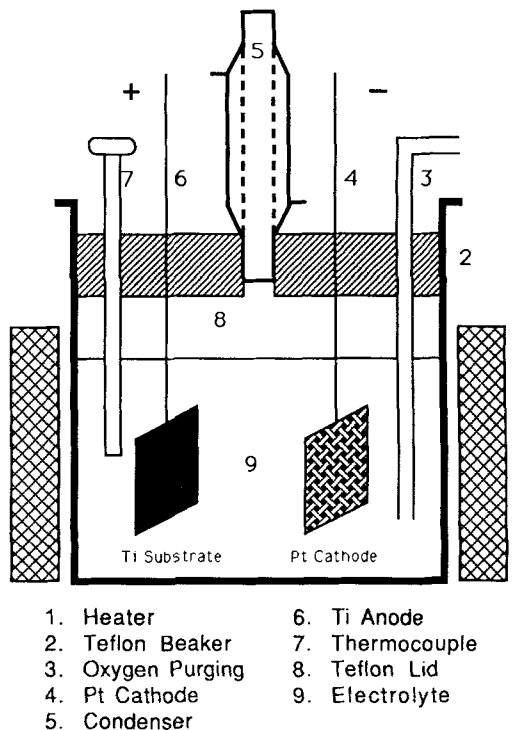


Fig. 2. Schematic diagram of the electrochemical apparatus for the low-temperature synthesis of BaTiO₃ thin films in open vessels.

electrolyte on the formation of BaTiO₃ films. NaOH as a 2M solution was used to achieve the desired pH. Atmospheres of ambient air, N₂, and O₂ were also evaluated. Electrolyte solutions were prepared by preheating the sodium hydroxide to remove dissolved CO₂ and then adding the Ba²⁺ salt. Prior to anodic deposition, electrolyte solutions were purged for 24 h with the desired atmosphere.

After each experiment, the coupons were washed in water adjusted to pH 9–10 with NH₄OH, rinsed in 2-propanol or ethanol, and air-dried prior to characterization. Samples were stored in covered containers in a desiccator prior to characterization. Care was taken to expose the samples to the ambient environment for as short a time as possible during handling to minimize BaCO₃ formation.

Characterization of electrothermally prepared BaTiO₃ thin films was performed in the Major Analytical Instrumentation Center (MAIC) at the University of Florida. X-ray diffractometry (XRD, APD3720, CuKα, fine tube, 40kV–20 mA, Philips Electronics, Mahwah, NJ), scanning electron microscopy (SEM, JSM6400, JEOL, Boston, MA), transmission electron microscopy (TEM, JEOL200CX, JEOL), and Auger electron spectroscopy (AES, PHI660, Perkin-Elmer, Eden Prairie, MN) were used to characterize the structural, compositional, and topographical features of the BaTiO₃ thin films. XRD was performed on the washed and dried samples using CuKα radiation and a scanning rate of 2.4°/min from 10° to 70° 2θ. SEM photomicrographs were obtained on uncoated samples. During SEM analysis, energy-dispersive analysis for X-rays was performed with an ultrathin window for light elements (UTW, Tracor Northern, Dallas, TX) to verify the presence of Ba, Ti, and O in each of the samples. Samples for TEM analysis were prepared by mechanically polishing the treated coupons on one side to about 75-μm thickness and subsequently cut into 3-mm-diameter disks using an ultrasonic disk cutter. The disk samples were then dimpled on the polished side to obtain a central thickness of about 15 μm and, finally, back-thinned employing Ar-ion milling at room temperature to remove Ti substrate at the center of the sample. The milled samples were coated with carbon to improve conductivity. Bright-field imaging and selected area diffraction (SAD) studies were performed on the central

Table I. Electrochemical Synthesis Conditions and Characterization Data for Selected BaTiO₃ Thin Films

Sample No.	Temp (°C)	Time (h)	pH	Current (mA/cm ²)	Electrothermal history		XRD analysis, phases	SEM analysis, grain size (μm)	AES analysis, chemistry	Film thickness (μm)
					Solution	Atmosphere				
1	100	53	13.75	0.5	0.5M Ba(OH) ₂ ·8H ₂ O	Ambient	BaTiO ₃ [*] , BaCO ₃	0.2–0.5	BaCO ₃ on surface, subsurface BaTiO ₃ revealed after sputtering	0.4
2	100	48	12.25	0.5	0.5M Ba(CH ₃ COO) ₂ + NaOH	N ₂ reflux	BaTiO ₃ , TiO ₂ [*] , TiO ₂	NA	TiO ₂ /TiO as dominant phases, BaCO ₃ close to surface	0.03
3	100	30	13.25	0.5	0.5M Ba(CH ₃ COO) ₂ 1M NaOH	O ₂ reflux	BaTiO ₃ [*] , BaCO ₃	0.2–0.5	Thick, uniform BaTiO ₃ film	0.4
4	100	4	13.50	0.5	0.5M Ba(CH ₃ COO) ₂ 2M NaOH	O ₂ reflux	BaTiO ₃ [*] , BaCO ₃	0.1–0.25	Homogeneous, uniform film	0.2
5	100	4	13.75	No current	0.5M Ba(CH ₃ COO) ₂ 2M NaOH	O ₂ reflux	BaTiO ₃ [†]	0.1–0.15	Very thin film of BaTiO ₃	0.1
6	100	24	13.75	1.25	0.5M Ba(CH ₃ COO) ₂ 2M NaOH	O ₂ reflux	BaTiO ₃ [†]	0.1–0.25	Slightly thicker film with no surface contamination	0.1
7	55	24	13.75	1.25	0.5M Ba(CH ₃ COO) ₂ 2M NaOH	O ₂ reflux	BaTiO ₃	0.2–1.0	Very thick, continuous film, bimodal grain size	0.6
8	55	24	13.75	2.50	0.5M Ba(CH ₃ COO) ₂ 2M NaOH	O ₂ reflux	BaTiO ₃	0.2–1.0	Thinner film, continuous, bimodal grain size	0.5
9	29	24	13.75	1.25	0.5M Ba(CH ₃ COO) ₂ 2M NaOH	O ₂ reflux	Unknown	2.0–3.0	No continuous film, discrete particles	Not applicable

*Dominant phases. Ti was found in all XRD patterns. †AES analysis showed the presence of a very thin layer of BaCO₃ on surface, probably formed during the postsynthesis handling of the films.

thin regions of the samples using a 200-kV accelerating voltage (electron beam wave length $\lambda = 0.0251 \text{ \AA}$) and 820-mm camera length (L). The SAD patterns were indexed by measuring the distance (R) between individual spots and rings, using a magnifier lens with an accuracy of $\pm 0.1 \text{ mm}$. The d -spacings for various sets of crystallographic planes were calculated using the formula $Rd_{hkl} = L\lambda$.

AES was performed using a 10-kV electron beam to determine the near-surface composition of the films. Argon ions accelerated at 3 kV on a 3-mm by 3-mm area were used to remove layers of material to obtain a compositional profile of the film as a function of depth into the film. The sputter rate was estimated to be 10 nm/min. The films were incrementally sputtered at 30-s intervals (~ 5 -nm depths) and AES performed until the titanium substrate was reached to obtain composition as a function of depth through the film. All films in which BaTiO₃ is present also have an underlying layer of TiO₂ or TiO, indicated by XRD and AES analyses. Therefore, BaTiO₃ film thickness was defined as the midpoint between the sputter times at which Ba and Ti cross over and Ti and O cross over. For example, in Fig. 3(C), the Ba and Ti cross over in the compositional profile at ~ 38 min, corresponding to about 380 nm, and Ti and O intersect at ~ 68 min, corresponding to 680 nm. The BaTiO₃ film thickness is taken as the midpoint between these two values at 53 min, or about 530 nm. The relatively small contribution in overall thickness produced by any BaCO₃ on the surfaces of the films was ignored in the calculation of BaTiO₃ film thickness.

Whether the films were continuous or contained pores and fissures was determined by electrical resistivity measurements in conjunction with SEM photomicrographs of the microstructure. Films were electroded by placing a mask with a regular array of holes over the film and sputter-coating a Au/Pd film or painting on silver electrodes. The silver electrodes could be subsequently washed from the film with a suitable solvent such as acetone, and the films were used for further analysis. The relative resistivity of each film was determined with a standard electrometer and electrical probes.

IV. Results and Discussion

The formation of polycrystalline BaTiO₃ thin films on titanium substrates has been observed under a variety of electrothermal conditions. Table I gives the experimental conditions and some of the relevant physical characteristics of selected films. Visual examination of the thinner films indicates the presence of multiple interference patterns of yellow, blue, and purple, as previously reported.^{5,6} The films with thicknesses of about 0.2 μm are typically reflective and transparent, whereas thicker films are dark gray and optically opaque. The characteristics of the synthesized BaTiO₃ thin films are dependent on the processing conditions as discussed below.

(1) Phase Stability of the BaTiO₃ Films

The phases present in the films were evaluated as a function of the starting electrolyte, atmosphere, solution pH, and temperature. BaTiO₃ thin films were initially synthesized in 0.5M Ba(OH)₂·8H₂O at 100°C, for periods up to 53 h as reported in previous studies.^{1–6} These conditions produce dark-gray BaTiO₃ films contaminated with BaCO₃ (sample 1). Reagent grade Ba(OH)₂·8H₂O is inherently contaminated with BaCO₃ ($\sim 2 \text{ wt\%}$). A CO₃²⁻-free Ba²⁺ solution was more easily achieved with Ba(CH₃COO)₂ as the electrolyte. Representative XRD traces are given in Fig. 4 for samples 6 and 7 synthesized at 100° and 55°C, respectively. BaCO₃ in samples 3 and 4 was attributed to the reaction of atmospheric CO₂ with the aqueous, alkaline electrolyte film covering the sample surface at the time of removal from vessel. The surface contamination by BaCO₃ was minimized in samples 5 through 9 by careful

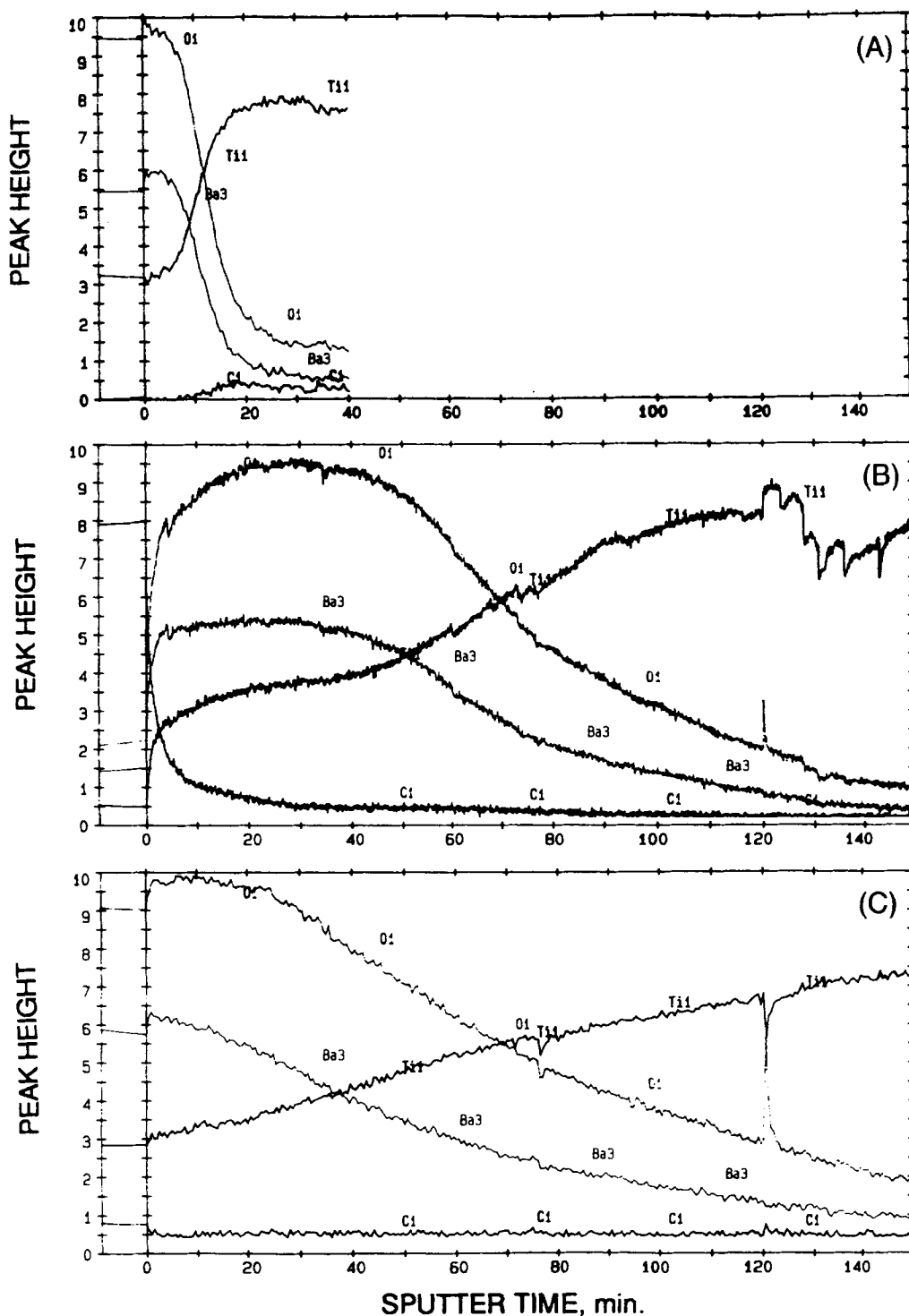


Fig. 3. Auger spectroscopy data for the thin films synthesized at (A) 100°C (sample 6), (B) 55°C and low current density (sample 7), and (C) 55°C and high current density (sample 8) showing variation in film thickness as a function of temperature and current density.

washing with CO_2 -free, ammoniated water at $\sim\text{pH } 9$, followed by a rinse with 2-propanol or ethanol.

The atmosphere also has a strong effect on the phase purity of the film. Electrothermal syntheses in an ambient atmosphere produced a mixture of BaTiO_3 and BaCO_3 . Both the atmosphere and pH were varied in the preparation of sample 2. Nitrogen was evaluated as an atmosphere to minimize the formation of the carbonate salt. The pH was also decreased to determine if BaTiO_3 would form or TiO_2 as predicted in Fig. 1. Both TiO_2 and possibly a poorly crystallized form of BaTiO_3 are present in sample 2 as shown in Fig. 5. However, the basis for the presence of BaTiO_3 is only the poorly crystallized (100)

peak at $22^\circ 2\theta$. Furthermore, the combination of the N_2 atmosphere and lower pH also leads to a reduced form of Ti(II) as TiO . Therefore, samples in subsequent experiments were produced using an O_2 atmosphere and at elevated pH values.

The role of oxygen in the process of thin-film formation is not fully understood. However, the presence of O_2 facilitates the formation of BaTiO_3 at low temperatures. It is possible that O_2 either is physically adsorbed at the metal/electrolyte interface to promote oxide formation or provides an oxidizing medium, itself getting reduced at the oxide/electrolyte interface to generate an excess of OH^- ions or H_2O_2 , resulting in a change in local pH and ionic equilibria. If the local environment is

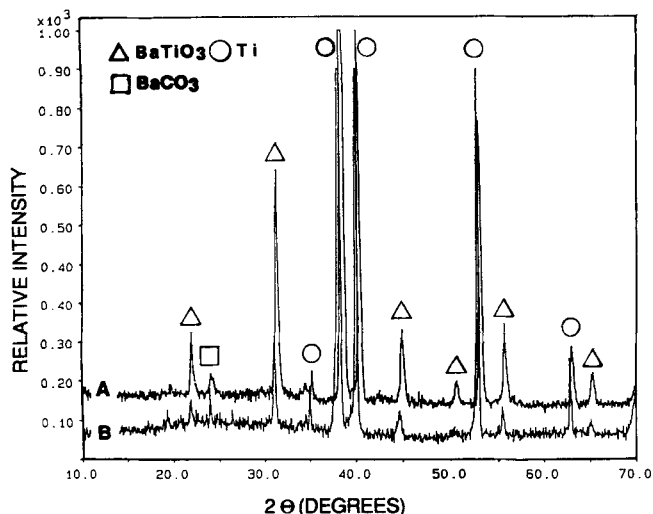
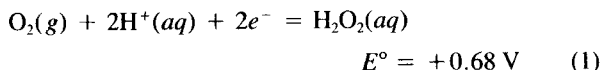


Fig. 4. Comparison of X-ray diffraction data for the thin films synthesized at (A) 55°C (sample 7), and (B) 100°C (sample 6).

changed because of OH⁻ or H₂O₂ generation, then the efficiency of dissolution-precipitation reactions will govern the product of anodization. Oxygen can react to form H₂O₂ under the conditions in which all experiments have been performed in the current work via reactions such as³⁰



The electrochemical conditions leading to Ti(IV), a valence state suitable for BaTiO₃ formation, may be promoted by complex ion formation with H₂O₂. The formation of Ti-H₂O₂ complexes elevates the solubility of Ti(IV)³¹ and, thus, may provide a greater driving force for the deposition of BaTiO₃. Alternatively, the peroxide may promote the formation of BaO₂ at lower temperatures. The implications of this latter effect are discussed below. A calculation of ionic equilibria that incorporates all of these various electrochemical scenarios is beyond the scope of the current work but will be addressed in future studies.

Solution pH also has a strong role in controlling the formation of phase-pure BaTiO₃. As shown in Fig. 1, BaTiO₃ is the stable phase only at solution pH values greater than ~pH 12. The theoretical phase stability is verified by the XRD pattern in Fig. 5 for the film formed under N₂ atmosphere at pH 12.25 (sample 2), which shows only a poorly crystalline BaTiO₃ associated with TiO and TiO₂ as the predominant phases, whereas the most phase-pure BaTiO₃ films (samples 5-8) have been formed in solutions with pH values greater than 13 and with an

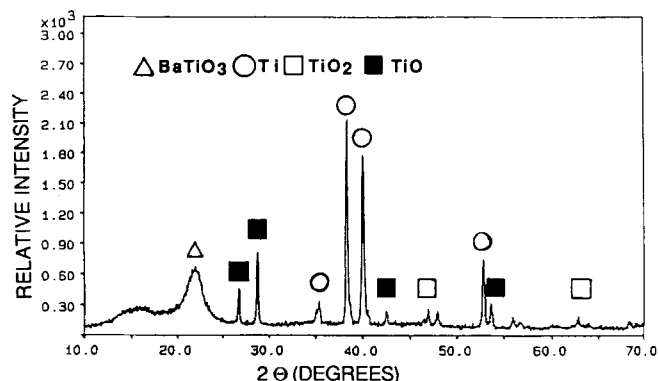


Fig. 5. X-ray diffraction data for the thin film (sample 2) synthesized at pH 12.25. Titanium oxides are the predominant phases.

O₂ reflux. These data support, but not conclusively, the hypothesis that, under highly alkaline conditions, the presence of Ba²⁺ in solution promotes the formation of crystalline BaTiO₃(s) as the most stable phase, with an amorphous titanium oxide acting as the intermediate phase. This observation is consistent with Prusi and Arsov,¹¹ who recently reported the formation of X-ray-amorphous titanium oxide on titanium surfaces in highly alkaline solutions under open-circuit conditions.

There is a minimum temperature at which continuous BaTiO₃ films will form within 24 h. BaTiO₃ films have been synthesized within 4 h at 100°C (e.g., samples 4 and 5, Table I). BaTiO₃ films are formed within 24 h at 55°C. Shorter synthesis times at 55°C have not yet been evaluated. However, continuous BaTiO₃ films are not formed within 24 h at 29°C, based on the characteristics of sample 9. No BaTiO₃ has been detected using XRD even with slow scans across the major XRD peaks for sample 9. Thus, at least for 24-h reaction times, there is a minimum temperature between 55° and 29°C at which BaTiO₃ will form. Regardless, the conditions promoting the formation of BaTiO₃ films at 55°C indicate validity of the theoretical approach summarized in Fig. 1 for 25°C to guide the development of the low-temperature synthesis of BaTiO₃. The short reaction times relative to those required for the homogeneous formation of BaTiO₃ particles^{19,24} at similar temperatures also support the thesis that a heterogeneous surface is required to synthesize BaTiO₃ at low temperatures in aqueous solutions.

(2) Thickness, Grain Size, and Porosity of the BaTiO₃ Films

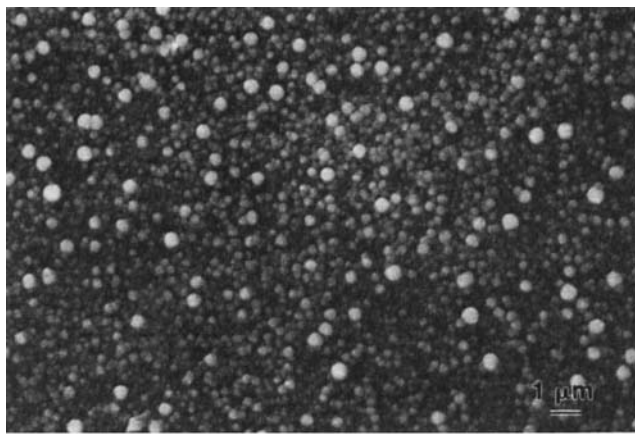
Microstructural characteristics of the phase-pure BaTiO₃ films, particularly samples 5-8, are strongly influenced by the current density and temperature at which a particular film is synthesized. In general, the current density has less influence on film thickness at 100° than 55°C. For example, sample 5 prepared at 100°C without an applied current had a BaTiO₃ film thickness of about 0.1 μm, while sample 6 prepared at 100°C with 1.25-mA·cm⁻² current density had only a modest increase in thickness to 0.2 μm. However, it is obvious from the AES compositional profile data for samples 6, 7, and 8 summarized in Fig. 4 that lower temperatures and not current density have the most profound effect on film thickness. Film thicknesses approaching 1 μm were obtained at 55°C (samples 7 and 8) in contrast to films in the range of 0.2 μm synthesized at 100°C.

Thickness of the films corresponds to the size of grains observed in SEM photomicrographs shown in Fig. 6. Estimates of the thickness of films based on SEM analysis of either grain size or cross-sectional views are erroneous because of the underlying TiO₂ films leading to an overestimate of the actual BaTiO₃ film thickness. Compositional profile analysis by AES or X-ray photon spectroscopy provide more accurate estimates of the ferroelectric film thickness. The diameter of the uniform grains in sample 4 synthesized at 100°C are approximately 0.2 μm, while the grain diameter in sample 7 synthesized at 55°C range from 0.2 μm to greater than 1 μm. The large grains in sample 9 synthesized at 29°C are similar to those present in sample 7, as shown in Fig. 7. However, there are no fine grains obvious in the microstructure of sample 9. The bimodal grain size distribution indicates that there are two pathways for grain formation as discussed below.

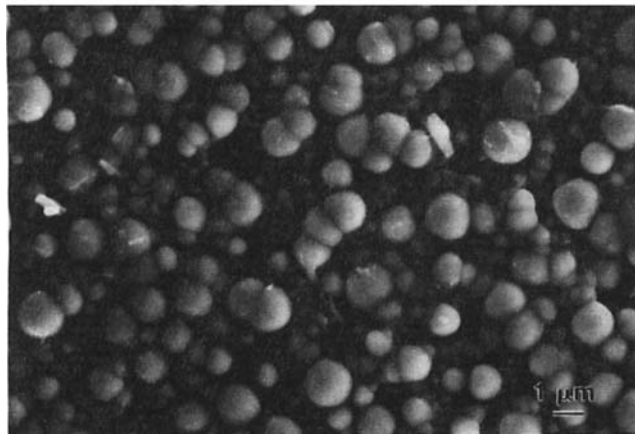
The degree of porosity indicated by the electrical resistivity of the films is also dependent on synthesis temperature. All films, except those prepared at 55°C with the bimodal grain sizes, had pores and fissures which provided electrically conductive pathways and very low resistivities. In contrast, samples 7 and 8 prepared at 55°C are electrically resistive. Capacitance and the dielectric loss factor will be reported at a later time, but it is expected that a static dielectric constant as low as 300, similar to that of other electrothermally synthesized films, will be found because of the relatively fine grain size.³²

(3) Discussion of Film Formation Mechanisms

The kinetic studies necessary to determine the rate-limiting step(s) specific to the formation of BaTiO₃ films have not yet been performed. However, based on a knowledge of the corrosion behavior of titanium, the hydrothermal synthesis of



(A)



(B)

Fig. 6. Scanning electron micrographs of the surfaces of the thin films synthesized at (A) 100°C (sample 4) and (B) 55°C (sample 7). Additional details for the synthesis are provided in Table I.

BaTiO₃, and the current work, a film formation mechanism is proposed that accommodates both the literature and the data developed from the current study. The microstructural and AES compositional profile data suggest two distinct mechanisms based on the synthesis temperature that control film formation.

It is proposed that the formation of BaTiO₃ films is controlled by three distinct, but interrelated, processes:

(1) The rapid formation of either a Ti oxide or Ti hydroxide film, whose crystallinity and composition depend on the

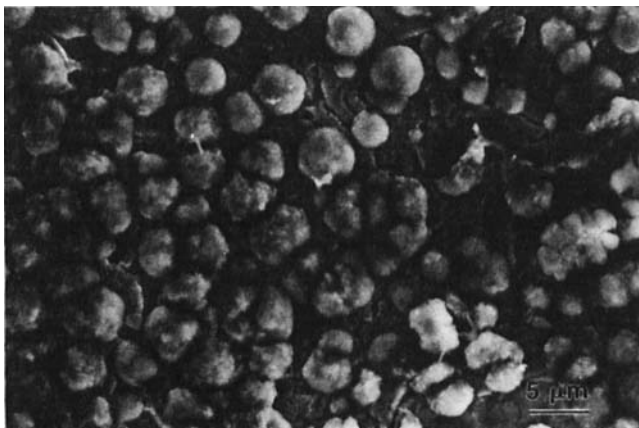


Fig. 7. SEM photomicrograph of sample 9 prepared at 29°C, showing large, discrete particles.

solution chemistry, atmosphere, and reaction temperature as discussed earlier.

(2) Nucleation of fine barium titanate crystallites on the surface of the amorphous, metastable Ti oxide film (formed under highly alkaline conditions), and their further growth to constitute an insulating, polycrystalline film of barium titanate.

(3) Concurrent with 1 and 2, the dielectric breakdown of the films if the voltage exceeds a critical value or range of values.

Titanium belongs to an important group of metals known as “valve metals” which have a large driving force to react with water to form metal oxides or hydroxous oxides.^{10,11} AES compositional profiles on the as-polished titanium coupons indicate a TiO₂ layer 10–20 nm thick. Thicker oxide layers form when an anodic current is passed across these metals. As shown in Fig. 3, a TiO₂ layer approximately 0.1 to 0.2 μm is present in the anodized films. These results are consistent with a recent report by Prusi and Arsov¹¹ on the growth kinetics of films formed on Ti under alkaline conditions. Based on kinetic analyses of film formation in alkaline solutions under open-circuit conditions and *in situ* ellipsometry measurements as a function of time, Prusi and Arsov showed that Ti hydroxous oxide films formed at 25°C within 100 min after an initial dissolution of the native TiO₂ layer. The initial dissolution period ranged from less than 1 min in 10M KOH to ~20 min in 1M KOH. In the conditions most closely approximating the present study, the Ti hydroxous oxide film grew to a thickness of approximately 60 nm. In correspondence with Pourbaix’s analysis,³⁰ Prusi and Arsov maintained that metastable Ti(OH)₃ was formed initially, but transformed electrochemically to TiO₂·H₂O with time. This secondary oxidation from Ti³⁺ to Ti⁴⁺ has not been observed in the current studies with the anodic polarization on the Ti coupon. Furthermore, the elevated temperatures used to prepare some of the samples (at 55° and 100°C) promote the formation of the rutile, anhydrous phase of TiO₂ under hydrothermal conditions.³³ The elevated temperatures used in the current study, if consistent with the aqueous phase equilibria of TiO₂ deduced from hydrothermal work, promote the formation of the anhydrous, crystalline material. Thus, based on the work of Prusi and Arsov and the current study, a relatively thick Ti hydroxous oxide or hydroxide film forms rather rapidly on the Ti surface within the first 100 min.

Hertl²⁶ has shown that it is likely that diffusion of Ba²⁺ into precursor TiO₂ particles is the rate-limiting step in the synthesis of BaTiO₃ particles. However, the low synthesis temperature of the crystalline BaTiO₃ films (55°C) formed in aqueous solutions and the relatively short times (as low as 4 h) compared to the much longer times (i.e., greater than 48 h) required for the synthesis of particles under similar conditions^{19,24,26} suggest that the crystallization of BaTiO₃ is augmented by a faster growth mechanism in the electrochemical process. Also, the diffusion of Ba²⁺ into the Ti oxide or Ti hydroxide under electrochemical conditions seems less likely, since the transport process would have to overcome the repulsion of the electric field on the anode.

In contrast, nucleation and growth of BaTiO₃ particulates in the electrochemical process is strongly supported by both microstructural data and the relatively rapid formation of the barium titanate films on the Ti substrates. The bright-field transmission electron image and the selected area diffraction (SAD) pattern (taken from the region close to the substrate) of the film prepared at 55°C (sample 7) shown in Fig. 8 indicate the presence of very fine BaTiO₃ crystallites embedded in a poorly crystalline TiO₂ film. These crystallites continue to grow into large BaTiO₃ grains seen as large, dark areas in the micrograph. This is supported by the presence of various BaTiO₃ spots and diffuse rings belonging to TiO₂ in the SAD pattern. Ion-milling conditions employed during the TEM sample preparation might have promoted partial crystallization of the originally amorphous Ti oxide film on the substrate. Based on this analysis, it is believed that the formation of BaTiO₃,

involves heterogeneous nucleation in a local environment provided by the electrochemical process in which the activity of Ti^{4+} or related Ti-hydroxide complex ions is high enough to react with Ba^{2+} in solution.

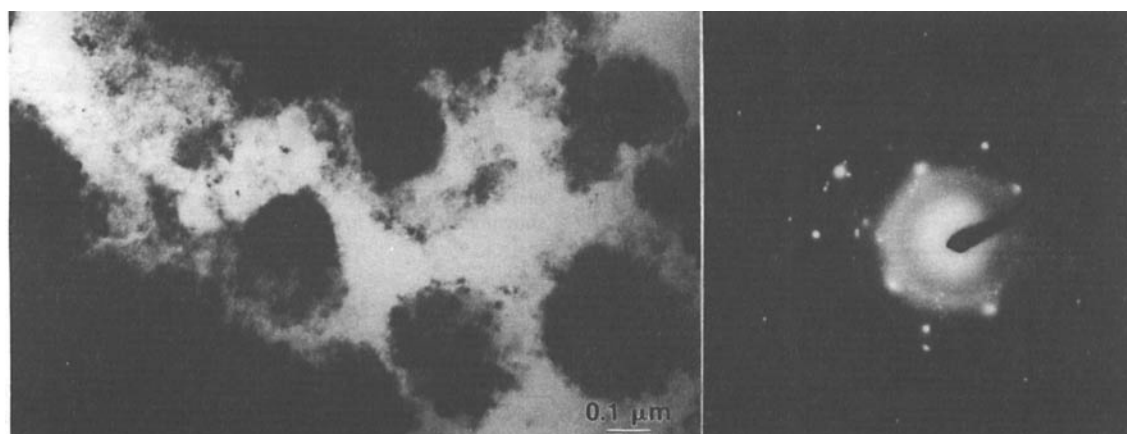
As the insulating oxide film grows at the anode, there is a steady increase in the voltage to accommodate the increase in resistance under galvanostatic conditions (i.e., constant current) across the growing film. As the film becomes thicker, further passage of anodic current can result in dielectric breakdown of the film, resulting in metal dissolution, oxygen evolution, or oxidation of species in the electrolyte. This behavior is consistent with the voltage oscillations as a function of reaction time shown in Fig. 9.

The voltage required to break down the TiO_2 and $BaTiO_3$ films in the current work indicates that dielectric breakdown is a factor in dictating the nature of the film. The dielectric breakdown strength for TiO_2 ranges from 2×10^4 to 1.2×10^5 $V \cdot cm^{-1}$, depending on the crystallographic direction of the applied voltage.³⁴ The breakdown strength for polycrystalline barium titanate³⁴ is approximately 1.17×10^5 $V \cdot cm^{-1}$. For either a TiO_2 or $BaTiO_3$ film thickness of 0.2 μm , these dielectric breakdown strengths correspond to applied voltages ranging from 0.4 to 2.4 V. The voltages as a function of time for selected samples summarized in Fig. 9 are consistent with the range of voltage expected for dielectric breakdown. However, temperature influences the range of voltages as well as the frequency of the breakdown with a greater oscillation in voltage present in the 100°C samples (from 1.5 to 3.5 V) than the 55°C

(from 1 to 2.5 V) or 29°C (1.75 to 2.5 V) samples. Furthermore, the cell voltages were relatively constant for the samples prepared in the latter two temperatures after about 10 h, while the sample at 100°C required 20 h to achieve a stable voltage. At present, it is uncertain how the microstructure changed with time during the deposition. Future studies will include these kinetic aspects of film formation.

The $BaTiO_3$ films fabricated by the "electrothermal" process at 100°C appear to be continuous and compact in the scanning electron micrographs. However, the high electrical conductance indicates the films synthesized at 100°C contain "shorts" or porosity. During the formation of the anodic oxide, stresses are produced at a metal/oxide interface which result in dielectric breakdown and induce fissures through the insulating layer. The evaluation of the physical nature, size, and distribution of these "shorts" by a voltage contrast method in SEM³⁵ is in progress.

The major microstructural difference between the films formed at 100°C and those formed at 55°C are the large grains present in the latter samples. It is currently believed that the large grains form at fissures created by the dielectric breakdown of the films. The hemispherical deposits physically fill the fissure, thereby preventing electrical current to flow. This contention is supported by the hemispherical deposits formed at 29°C, where $BaTiO_3$ is not found. The native oxide layer is still subject to dielectric breakdown as shown in Fig. 9, although the magnitude of the oscillations in voltage is significantly smaller than that present in the 55° or 100°C samples. Furthermore, the



Diffraction data from the SAD pattern:

Calculated d_{hkl}	Reference data d_{hkl}	Intensity	$h k l$
<hr/>			
Spots	JCPDS-ICDD	$BaTiO_3$	Ref. Pattern # 31-174
2.84±0.04	2.850	100	1 1 0
2.32±0.03	2.328	30	1 1 1
1.99±0.02	2.016	35	2 0 0
1.65±0.02	1.6445	25	2 1 1
<hr/>			
Rings	JCPDS-ICDD	TiO_2	Ref Pattern # 35-88
3.05±0.05	3.11	90	0 0 2
2.06±0.02	2.073	70	0 0 3

Fig. 8. Bright-field transmission electron image and the selected area diffraction pattern of the $BaTiO_3$ thin film prepared at 55°C (sample 7), showing the fine crystallites of $BaTiO_3$ embedded in a poorly crystalline TiO_2 film and surrounded by the fully grown $BaTiO_3$ grains seen as large, dark areas.

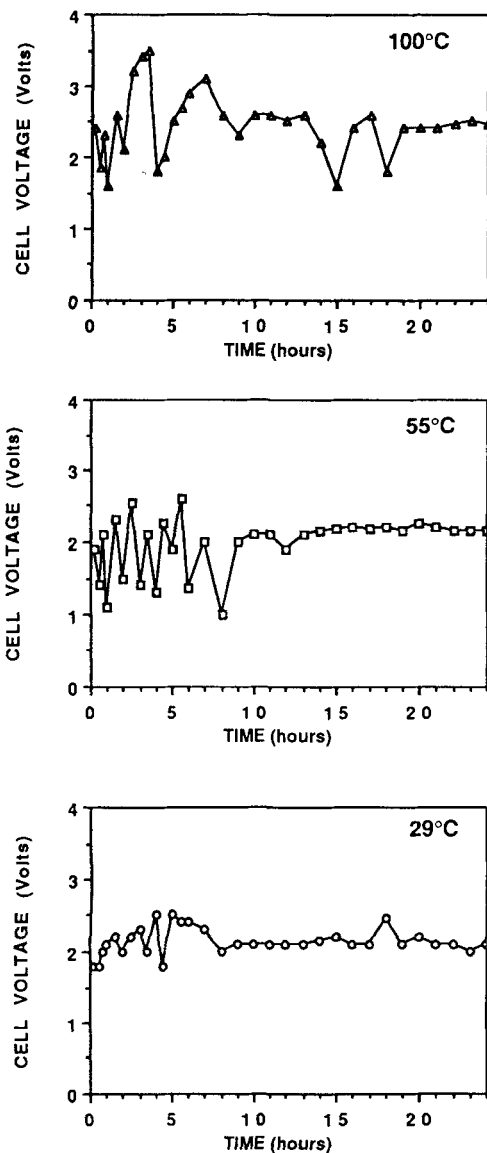


Fig. 9. Cell voltage as a function of time for samples prepared at 100°C (sample 6), 55°C (sample 7), and 29°C (sample 9). Electrothermal conditions for all samples were similar, other than the temperature.

oscillations in voltage indicating the cycle of deposition and breakdown is continuing are still experienced in the 100°C sample for times as long as 20 h, while the oscillations have basically ceased within 10 h for the 55° and 29°C samples.

The precise nature of the large grains in samples prepared at 55° and 29°C is unknown. Energy-dispersive analysis for X-rays performed with an ultrathin window for light elements indicates the deposits in sample 9 prepared at 29°C contain oxygen, barium, and titanium. However, at least some of the latter element is from the underlying TiO₂ and Ti layers. Argon sputtering on the surface of sample 9 shown in the SEM photomicrographs in Fig. 10 resolves some of the ultrastructure of the hemispherical deposits. The sputtered sample reveals that the hemispherical deposits are composed of elongated structures that may be related to the crystallographic orientation in the deposit. It is unlikely that the elongated structures in the argon-milled hemispherical structures are due to a phenomenon similar to that which leads to sputter-induced cone formation observed in ion-milled polycrystalline metal surfaces.³⁶ Energy-dispersive analysis with an ultrathin window for light-element detection indicates that the ion-milled deposits are still composed of Ba, O, and Ti, although again the latter may be

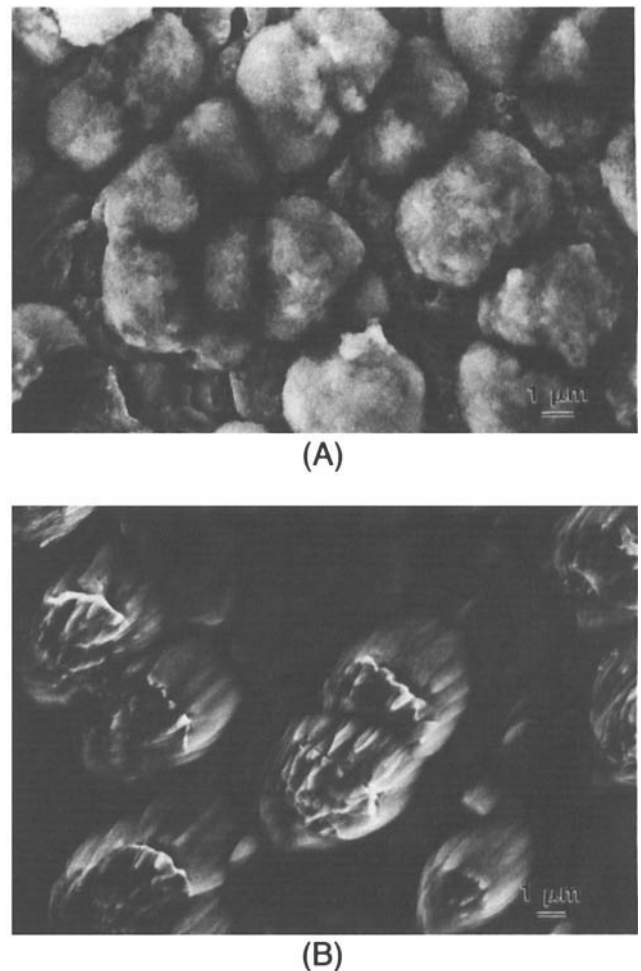


Fig. 10. SEM photomicrographs of large deposits on sample 9 prepared at 29°C: (A) before argon milling and (B) after argon milling, showing the texture in the hemispherical deposits.

due primarily to the substrate. Thus, it is believed that the milling reveals the crystallographic orientation or texture in the large deposits.

It is possible that the X-ray-amorphous, hemispherical deposits are a barium-titanium hydrous oxide, or alternatively, barium oxide or barium peroxide if the Ti indicated by the microanalysis is due to the underlying substrate. In any case, the validity of the following formation scheme can be more rigorously tested in future experiments:

(1) The Ti oxide layer forms rapidly upon introduction of the Ti coupon into solution. The thickness of this layer is dictated to some extent by the current density on the Ti anode.

(2) The nucleation and growth of the BaTiO₃ layer is dictated by the nature of the Ti oxide layer, solution chemistry, and the atmosphere.

The formation rate of the BaTiO₃ particles under hydrothermal conditions follows a parabolic rate law as developed by Hertl.²⁶ This scheme is also consistent with the well-established mechanistic models for the diffusion-controlled growth of the anodic films.³⁷ The growth rates for the electrochemically prepared BaTiO₃ films can be evaluated against these models, particularly those associated with the anion diffusion and point defects,³⁷ to elucidate different stages of the film formation. It is currently believed that one of these reaction mechanisms leads to the formation of the 0.2- μ m grains and small pores observed in the films synthesized at 100°C.

Acknowledgments: The authors thank the Department of Materials Science and Engineering, University of Florida, Gainesville, for the financial support and use of its facilities, including the Major Analytical Instrumentation

Center (MAIC). Special thanks are extended to Mr. Richard Crockett and to Dr. Eric Lambers for the operation of MAIC equipment and for valuable insight in the characterization of the films.

References

- ¹S.-E. Yoo, M. Yoshimura, and S. Somiya, "Direct Preparation of BaTiO₃ Powders from Titanium Metal by Anodic Oxidation under Hydrothermal Conditions," *J. Mater. Sci. Lett.*, **8**, 530-32 (1989).
- ²M. Yoshimura, S.-E. Yoo, M. Hayashi, and N. Ishizawa, "Preparation of BaTiO₃ Thin Film by Hydrothermal-Electrochemical Method," *Jpn. J. Appl. Phys.*, **28** [11] L2007-L2009 (1989).
- ³S.-E. Yoo, M. Hayashi, N. Ishizawa, and M. Yoshimura, "Preparation of Strontium Titanate Thin Films on Titanium Metal Substrate by Hydrothermal-Electrochemical Method," *J. Am. Ceram. Soc.*, **73** [8] 2561-63 (1990).
- ⁴Y. Sakabe, Y. Hamaji, M. Hayashi, Y. Ogino, N. Ishizawa, and M. Yoshimura, "Synthesis of SrTiO₃ and CaTiO₃ Thin Films by Hydrothermal-Electrochemical Method"; presented at the Fifth U.S.-Japan Seminar on Dielectric and Piezoelectric Ceramics, Kyoto, Japan, December 11-14, 1990.
- ⁵N. Ishizawa, H. Banno, M. Hayashi, S.-E. Yoo, and M. Yoshimura, "Preparation of BaTiO₃ and SrTiO₃ Polycrystalline Thin Films on Flexible Polymer Film Substrate by Hydrothermal Method," *Jpn. J. Appl. Phys.*, **29** [11] 2467-72 (1990).
- ⁶K. Kajiyoshi, N. Ishizawa, and M. Yoshimura, "Preparation of Tetragonal Barium Titanate Thin Film on Metal Substrate by Hydrothermal Method," *J. Am. Ceram. Soc.*, **74** [2] 369-74 (1991).
- ⁷Metals Handbook, 9th ed., Vol. 5, *Surface Cleaning, Finishing, and Coatings*. ASM International, Materials Park, OH, 1982.
- ⁸R. J. Philips, M. J. Shane, and J. A. Switzer, "Electrochemical and Photoelectrochemical Deposition of Thallium (III) Oxide Films," *J. Mater. Res.*, **4** [4] 923-29 (1989).
- ⁹A. E. Feuersanger, A. K. Hangenlocher, and A. L. Solomon, "Anodic TiO₂ Thin Films," *J. Electrochem. Soc.*, **111**, 1387 (1964).
- ¹⁰L. Young, *Anodic Oxide Films*; pp. 253-57. Academic Press, New York, 1961.
- ¹¹A. R. Prusi and Lj. D. Arsov, "The Growth Kinetics and Optical Properties of Films Formed under Open Circuit Conditions on a Titanium Surface in Potassium Hydroxide Solutions," *Corros. Sci.*, **33** [1] 153-64 (1992).
- ¹²K. Osseo-Asare, F. J. Arriagada, and J. H. Adair, "Solubility Relationships in the Coprecipitation Synthesis of Barium Titanate: Heterogeneous Equilibria in the Ba-Ti-C₂O₄-H₂O System"; pp. 47-53 in *Ceramic Transactions*, Vol. 1, *Ceramic Powder Science II*. Edited by G. L. Messing, E. R. Fuller, Jr., and H. Hausner. American Ceramic Society, Westerville, OH, 1988.
- ¹³J. H. Adair, B. L. Utech, K. Osseo-Asare, and J. P. Dougherty, "Solubility and Phase Stability of Barium Titanate in Aqueous Suspension"; see Ref. 4.
- ¹⁴A. N. Christensen and S. E. Rasmussen, "Hydrothermal Preparation of Compounds of the Type ABO₃ and AB₂O₄," *Acta Chem. Scand.*, **17** [3] 845 (1970).
- ¹⁵A. N. Christensen, "Hydrothermal Preparation of Barium Titanate by Transport Reactions," *Acta Chem. Scand.*, **24** [7] 2447-52 (1970).
- ¹⁶S. Myhra, D. Savage, A. Atkinson, and J. C. Riviere, "Surface Modification of Some Titanate Minerals Subjected to Hydrothermal Chemical Attack," *Am. Mineral.*, **69**, 902-909 (1984).
- ¹⁷J. Menashi, R. C. Reid, and L. Wagner, "Barium Titanate Powders," U.S. Pat. No. 4 829 033, May 9, 1989.
- ¹⁸S. Kaneko and F. Imoto, "Synthesis of Fine-Grained Barium Titanate by a Hydrothermal Reaction," *Nippon Kagaku Kaishi*, **6**, 985-90 (1975).
- ¹⁹E. Lilley and R. Wusarika, "Method for the Production of Mono-Size Powders of Barium Titanate," U.S. Pat. No. 4 764 493 (1988).
- ²⁰J. Menashi, R. C. Reid, and L. P. Wagner, "Barium Titanate Based Dielectric Compositions," U.S. Pat. No. 4 832 939 (1989).
- ²¹K. Abe, M. Aoki, H. Rikimaru, T. Ito, K. Hidaka, and K. Segawa, "Process for Producing a Composition Which Includes Perovskite Compounds," U.S. Pat. No. 4 643 984, February 17, 1987.
- ²²T. R. N. Kutty and Vivekanandan, "Precipitation of Rutile and Anatase (TiO₂) Fine Powders and Their Conversion to MTiO₃ (M = Ba, Sr, Ca) by the Hydrothermal Method," *Mater. Chem. Phys.*, **19**, 533-46 (1988).
- ²³T. R. N. Kutty and P. Murugaraj, "Hydrothermal Precipitation and Characterization of Poly titanates in the System BaO-TiO₂," *J. Mater. Sci. Lett.*, **7**, 601-603 (1988).
- ²⁴M. K. Klee and H. W. Brand, "Method of Manufacturing Powdered Barium Titanate," U.S. Pat. No. 4 859 448 (1989).
- ²⁵W. Ovrachenko, L. Shvets, F. Ovcharenko, and B. Kornilovich, "Kinetics of Hydrothermal Synthesis of Barium Metatitanate," *Inorg. Mater.*, **15** [11] 1560-62 (1979).
- ²⁶W. Hertl, "Kinetics of Barium Titanate Synthesis," *J. Am. Ceram. Soc.*, **71** [10] 879-83 (1988).
- ²⁷A. G. Walton, *The Formation and Properties of Precipitates*. Kreiger Publishing, Huntington, NY, 1979.
- ²⁸C. H. P. Lupis, *Chemical Thermodynamics of Materials*; pp. 89-94. North-Holland, New York, 1983.
- ²⁹A. E. Nielsen, "Precipitates: Formation, Coprecipitation and Aging"; pp. 269-347 in *Treatise of Analytical Chemistry, Part I, Theory and Practice*; 2nd ed., Vol. 5. Edited by I. M. Kolthoff and P. J. Elving. Wiley, New York, 1983.
- ³⁰M. Pourbaix, *Atlas of Electrochemical Equilibria in Aqueous Solutions*, 2nd ed., pp. 213-22. National Association of Corrosion Engineers, Houston, TX, 1974.
- ³¹J. A. Connor and E. A. V. Ebsworth, *Inorganic Chemistry and Radiochemistry*; Vol. 6. Edited by H. J. Emeleus and A. G. Sharpe. Academic Press, New York, 1964.
- ³²R. Bacsa, P. Ravindranathan, and J. P. Dougherty, "Electrochemical, Hydrothermal, and Electrochemical-Hydrothermal Synthesis of Barium Titanate Thin Films on Titanium Substrates," *J. Mater. Res.*, **7** [2] 423-28 (1992).
- ³³E. F. Osborn, "Subsolidus Reactions in Oxide Systems in the Presence of Water at High Pressures," *J. Am. Ceram. Soc.*, **36** [9] 279-85 (1953).
- ³⁴G. C. Walther and L. L. Hench, "Dielectric Breakdown of Ceramics"; pp. 539-64 in *Physics of Electronic Ceramics*, Part A. Edited by L. L. Hench and D. B. Dove. Marcel Dekker, New York, 1971.
- ³⁵D. T. Y. Wei, "Identification of Ceramic Capacitor Shorts by Voltage Contrast in Scanning Electron Microscopy"; pp. 87-96 in *Advances in Ceramics*, Vol. 11, *Processing for Improved Productivity*. Edited by K. M. Nair. American Ceramic Society, Columbus, OH, 1984.
- ³⁶G. K. Wehner and D. J. Hajicek, "Cone Formation on Metal Targets during Sputtering," *J. Appl. Phys.*, **42** [3] 1145-49 (1971).
- ³⁷M. G. Fontana, *Corrosion Engineering*, 3rd ed.; pp. 474-81. McGraw-Hill, New York, 1987. □